Portable EEG in groups shows increased brain coupling to strong health messages

Martin A. Imhof [1 2 *], Karl-Philipp Flösch [1 2], Ralf Schmälzle [3], Britta Renner [1 2], & Harald T. Schupp [1 2 *]

[1] Department of Psychology, University of Konstanz, 78457 Konstanz, Germany
[2] Centre for the Advanced Study of Collective Behaviour, University of Konstanz, 78457 Konstanz, Germany
[3] Department of Communication, Michigan State University, East Lansing, MI 48824, USA
* Corresponding authors

Corresponding authors

Martin Imhof & Harald Schupp
Department of Psychology
University of Konstanz
PO Box 36
78457 Konstanz, Germany
E-Mail: martin.imhof@uni.kn & harald.schupp@uni.kn

Manuscript information

No. of pages:	30 (incl. author information, references & figure legends)
No. of figures:	4
No. of tables:	1

Abstract

Health messages are core building blocks of public health efforts. Neuroscientific measures offer insights into how target audiences receive health messages. To move towards real-word applications, however, challenges regarding costs, lab restraints, and slow data acquisition need to be addressed. Using portable EEG and inter-subject correlation (ISC) analysis as measure of message strength, we ask whether these challenges can be met. Portable EEG was recorded while participants viewed strong and weak video health messages against risky alcohol use. Participants viewed the messages either individually or in a focus group-like setting with six participants simultaneously. For both viewing conditions, three correlated components were extracted. The topographies of these components showed high spatial correlation with previous high-density EEG results. Moreover, ISC was strongly enhanced when viewing strong as compared to weak health messages in both the group and individual viewing condition. The findings suggest that ISC analysis shows sensitivity to message strength, even in a group setting using low-density portable EEG. Measuring brain responses to messages in group settings is more efficient and scalable beyond the laboratory. Overall, these results support a translational perspective for the use of neuroscientific measures in health message development.

Keywords

health communication, portable EEG, group, inter-subject correlation, ISC, alcohol

Introduction

Every day, we come across health messages on topics like smoking, nutrition, or risky alcohol use. Such mass media messages are crucial for public health efforts as mass media provides the ability to reach large populations through TV, radio, or online media (e.g., Rice & Atkin, 2013; Wakefield et al., 2010). However, there remains the challenge to design and select messages that effectively achieve campaign goals, such as impacting attitudes or health-related behavior. Health messages often use engaging audio-visual formats or stories to make them memorable and heighten individual risk perception. Typically, message development and selection is done by using self-report methods such as focus groups or surveys (Merton &

Kendall, 1946; Rice & Atkin, 2013). More recently, brain measures have also been used to examine affective and cognitive reactions to health messages (e.g., Falk, 2010; Imhof et al., 2017; Kaye et al., 2016; Schmälzle et al., 2020; Weber et al., 2014). Neuroscientific measures can complement self-report methods for assessing health message reception by providing process-based insights captured during the actual moment of reception. These measures do not rely on retrospective recall and can detect responses that may occur outside of conscious awareness (e.g., Falk et al., 2015; Weber et al., 2018). Furthermore, there is increasing evidence that neural measures contribute to the understanding of health behavior change, explaining variance beyond that accounted for by self-report measures (Berkman & Falk, 2013; Falk et al., 2015; Imhof et al., 2020).

The brain reactions to dynamic health messages can be assessed by a technique called inter-subject correlation analysis (ISC). ISC assesses how stimuli prompt similar brain responses across audience members, yielding a measure to quantify the impact of media messages (Hasson et al., 2010; Schmälzle, 2022). While other neural metrics assess brain activity at the individual level, ISC identifies the brain-to-brain commonalities among multiple subjects. Theoretically, ISC measures are ideal to assess health communication, because they provide an inherently audience-based metric of collective brain engagement, which aligns with the goal of mass communication efforts (Schmälzle, 2022). Methodologically, ISC measures have the advantage that they allow using fully naturalistic messages while circumventing the need for complex stimulus models or artificial control of stimulus features.

Previous research covering rhetoric, interpersonal communication, narratives, or movie viewing suggests that ISC levels during naturalistic stimulation relate to message strength, and affective and cognitive processing more generally (Hasson et al., 2012; Hasson et al., 2010; Jääskeläinen et al., 2021; Schmälzle, 2022; Schmälzle et al., 2015). The ISC method has also been employed in lab research on health communication. For instance, when participants viewed a video concerning the H1N1 swine flu in the fMRI scanner, individuals with high risk perception showed increased ISC in the anterior cingulate cortex compared to individuals with low risk perception, presumably reflecting increased responses to threatening information (Schmälzle et al., 2013). Most notably, enhanced ISC was observed to strong video health messages against risky alcohol use in the dorsomedial prefrontal cortex, precuneus, and the insulae, presumed to reflect increased affective stimulus processing, self-relevance, and attention towards salient stimuli (Imhof et al., 2017). Taken together, growing evidence suggests that ISC-based brain measurements provide insights in the dynamics of message reception and thus can help us understand how health messages impact audiences.

Despite these promising results, health communication neuroscience is still primarily a research tool and whether it has application potential remains an open question. Indeed, the translation of brain activity measurements from a pure research method into a useful tool for health message development and pre-testing faces many challenges. In medicine, this shift is often referred to as the "bench to bedside" problem, encompassing the journey from developing a drug, device, or procedure in the laboratory to its implementation in clinical or real-world settings (Drolet & Lorenzi, 2011; Wolf, 1974). Similarly, public health researchers distinguish between approaches that "can work" and those that "do work in practice" (Cochrane, 1972; Haynes, 1999). Considering this translational continuum, health communication neuroscience is still in the "bench" or "can work" mode.

Applied to the context at hand – using neural measures in message pre-testing - several challenges emerge: First, basic research relies on often expensive, complex techniques and lab environments. Translating this to practical applications necessitates cost-effective solutions that are feasible in non-lab or everyday situations. Second, basic research is typically time-consuming because data collection mostly happens one-participant-at-a-time. One way to overcome the data collection bottleneck is to collect data from multiple individuals together, combining social scientific focus group methods with neural measurements (e.g., Berns & Moore, 2012; Falk et al., 2010). If these challenges can be overcome, then neuroimaging might progress to a stage where it could support the development or selection of strong messages.

One technique that meets the requirements to overcome these challenges is EEG. Modern EEG amplifiers have become portable and more affordable. Indeed, research in educational and entertainment contexts demonstrates that it is possible to measure EEG in classroom, outdoors or in cinema settings (e.g., Barnett & Cerf, 2017; Dikker et al., 2017; Reinero et al., 2020; Zink et al., 2016). Moreover, the ISC approach to assess dynamic audio-visual stimuli has meanwhile also been extended to lab EEG (e.g., S. S. Cohen & Parra, 2016; Dmochowski et al., 2012; Madsen & Parra, 2022). A first study showed that EEG-ISC captured with low-density portable EEG during viewing engaging movies individually in a classroom setting was consistent with findings brought out with higher-density systems (Poulsen et al., 2017). Recently, we showed that strong health messages against risky alcohol use induced heightened EEG-ISC in a lab environment. In this work, we also used independent fMRI data to link the ISC findings not only to sensory-perceptual areas but also to the insula, the dorsomedial prefrontal cortex and further cortical midline regions - brain regions that have previously been associated with successful messaging (cf. Imhof et al., 2020).

The present study is an effort to move health communication neuroscience from a basic feasibility, or "can it work?"-stage, to a more practical implementation, or "does it work in practice?"-stage. To this end, we used a series of strong and weak video health messages against risky alcohol use. These messages previously elicited distinct differences in both, self-reported perceived message effectiveness, and synchronized brain reactions, as captured by fMRI- and EEG-ISC (Imhof et al., 2017, 2020). Here, we used portable EEG while presenting the messages to participants in two distinct ways: either individually, which resembled the conventional method, or in a group setting with six participants simultaneously viewing the messages. While more affordable, portable EEG comes with reduced spatial coverage and less sensors. Thus, one aim of the study was to test the reliability of ISC findings under these circumstances by using portable, 24-channel systems in a non-shielded everyday-like room to replicate previous findings from a stationary, 256-channel EEG within an electrically shielded lab environment (Imhof et al., 2020). In a first step, we determined whether portable systems can capture distinct correlated components in the EEG signal (Dmochowski et al., 2012; Parra et al., 2019) and whether the spatial topographies of these components match those from prior lab research. Next, we tested whether this setup could reveal increased brain synchronization among message recipients for strong as opposed to weaker messages, which was previously found during individual viewing with high-density lab EEG (Imhof et al., 2020). Finally, we assumed that similar results would emerge when conducting recordings within a more scalable group setting. Achieving alignment in results between EEG systems as well as the individual and group viewing condition are important prerequisites for translational applications and would support the use of neural measures in groups to explore the effectiveness of health messages.

Methods

Participants

The final sample included 41 participants (M_{Age} = 22.90, *SD* = 2.99, range: 18 to 32 years; 24 females, 17 males). 21 participants were measured in the group viewing condition while another 20 participants were measured in the individual viewing condition. Participants were eligible for the study if they reported drinking at least four alcoholic beverages per week. We assessed the participants' drinking behavior using the AUDIT alcohol screening questionnaire (range: 0 – 40; Babor et al., 2001). All participants in both viewing conditions exhibited risky drinking patterns (M_{Audit} = 11.10; *SD* = 4.76; range: 5 - 22) based on a cut-off recommendation for the German population (Rumpf et al., 2002). There were no significant differences across the two viewing conditions groups with respect to alcohol consumption (measured by means of AUDIT scores), age or gender ratio (AUDIT: $t(39)$ = 1.05, p = .30; M_{Group} = 11.86, *SD* = 4.23; $M_{\text{Individual}}$ = 10.30, *SD = 5*.25; Age: $t(39)$ = .87, p = .68, M_{Group} = 23.10 years, *SD* = 2.28; $M_{\text{Individual}}$ = 22.70 years, *SD* = 3.64, two-sided independent samples *t*-tests; 12 females per group). Furthermore, there were no significant differences in risk perception across the two participant groups (see Supplementary Methods).

All participants had normal hearing, normal or corrected-to-normal vision, and no history of neurological or psychological diseases. Data of four additional participants were excluded, due to intense signal artifacts at several sensors (*N* = 1), technical failure (*N* = 1), or not meeting predefined criteria for alcohol consumption or medication (*N* = 2). Excluded data were not analyzed. Sample size was based on the large effects observed in our previous work (Imhof et al., 2020) and based on the Covid-19 restrictions at the time of data collection, that is, it was possible to perform a total of four group measurements with six participants at a time. Power calculation (Faul et al., 2007) suggests that the empirical power of our study to find a moderate to large main effect of *Video Category*, was .88 to .99 (alpha = .95, f = .25 to .40) and to find a moderate two-way interaction effect of *Video Category* and *Viewing Condition* was .88 (alpha = .95, f = .25). All participants received course credit or monetary reimbursement.

Written informed consent was obtained according to the Declaration of Helsinki and the procedures were approved by the ethics committee of the University of Konstanz.

Materials

To create a strong and a weak health message category we used 10 of the most and 10 of the least effective messages of a larger database containing German-speaking video health messages against risky alcohol use. The same messages have been used in previous research and a more detailed description can be found in Imhof et al. (2017). Duration of the messages varied between 20 and 110 s and did not differ between the two categories ($t(18) = .43$, *n.s.*; $M_{\text{Strong}} = 58.5$ s, $SD = 25.93$; $M_{\text{Weak}} = 49.5$ s, $SD = 25.00$; independent samples *t*-test, two-sided). Basic physical features were assessed in our previous work, e.g., luminance, movement, or acoustic features, revealing no differences across the two message categories (Imhof et al., 2020). To control for effects of video length on EEG-ISC, we assessed potential relations between message length and ISC. As in our previous work (Imhof et al., 2020), there was no relation between length [in s] and EEG-ISC of any of the correlated components and neither for group nor individual viewing (Pearson's $rs = -.10$ to $.27$, all $ps > .25$).

Procedure

Prior to the experiments, we assessed EEG eligibility and collected self-report measures of drinking behavior as well as alcohol-related risk perceptions (t_1). In the main session, strong and weak health messages were presented in pseudo-randomized orders. In the group setting, six participants watched the video health messages, while sitting together in a semicircle in front of the screen (see Figure 1). Due to a no-show, one recording in the group viewing setting took place with five participants. In the individual viewing setting, one participant each viewed the messages in the same room. Seating positions were varied in the individual setting to resemble the seating positions in the group setting. In both viewing conditions, participants were asked to limit their movement during video viewing and instructed to freely and attentively view the videos, as in our previous and comparable ISC work using audio-visual stimuli. Additionally, in the group viewing condition, participants were instructed to refrain from talking during the videos. At least one researcher always remained in the back of the room to control stimulus presentation and EEG recordings. Due to Covid-19-related restrictions during the data collection period, participants in both viewing conditions wore face masks, limiting communication among participants.

We used Presentation software (Neurobehavioral Systems, Inc.) to present the videos and to synchronize EEG acquisition. Videos were wall-projected in front of the participants with a resolution of 800 * 450 pixels (projection size: 57 x 32 cm). The distance to the wall was approximately 270 cm yielding horizontal and vertical visual angles of about 12° x 7°. Sound was delivered via stereo speakers located in front of the participants. A three-second animated video fixation was presented prior to each health message. Participants were asked to attentively view the video health messages, without any further task instruction. After each video, a blank screen (ITI = 3.5 s) was presented. Overall, EEG measurements lasted for approximately 25 minutes.

Participants watched all messages again in randomized order in a separate block directly after the main session (t_2). For each video, participants provided single-item ratings regarding perceived effectiveness, argument strength and the amount of threatening or shocking content. Moreover, to track changes in alcohol-related risk perceptions and behavior, we collected self-report data prior to (t_1), directly after the main session (t_2), and in a four-week follow up online questionnaire (t_3). As in previous work, self-report items targeted at detailed alcohol consumption and risk perceptions were used. Contrasting to Imhof et al. (2020) there were no significant changes in risk perception and behavior (for details, see Supplementary Methods).

Figure 1 here

EEG acquisition and preprocessing

EEG and EOG scalp potential fields were measured with a 24-channel sensor cap (Smarting mobi EasyCap, mbt: mbraintrain.com; see Figure 1c). EEG data were sampled at 250 Hz using portable Smarting mobi amplifiers and recorded with Smarting Streamer acquisition software v3.4.3. Electrode impedances were kept below 10 kΩ, as recommended by manufacturer guidelines. Data was recorded continuously with the default reference FCz (Sensor CMS) and on-line filtered at the Nyquist frequency.

Data segments corresponding to the video health messages were extracted using the open-source signal processing toolbox EEGLAB and in-house MATLAB code. Offline preprocessing of EEG and EOG data was conducted based on prior work (e.g., S. S. Cohen & Parra, 2016; Dmochowski et al., 2012; Imhof et al., 2020; Parra et al., 2019). Specifically, EEG and EOG data were high-pass (0.5 Hz, IIR Butterworth filter, 6th order) and notch filtered (50 Hz, IIR Butterworth stopband filter, 49.5 & 50.5 Hz cutoffs). Eye movements were corrected by linearly regressing the approximate EOG channels (Fp1, Fp2, F7 & F8) from all other EEG channels. Outlier samples were identified in each channel, if their magnitude exceeded three times the interquartile range of the signal. Samples 40 ms before and after these outliers were replaced with zero values. Electrode channels with high variance (signal magnitude exceeding three times the interquartile range) were identified and replaced with zero values. These artifact rejection procedures were performed to discount outlier samples and channels in the subsequent calculation of covariance matrices, as ISC computation is sensitive to outliers (see also S. S. Cohen & Parra, 2016; Dmochowski et al., 2012; Parra et al., 2019).

EEG-ISC analysis

EEG-ISC analysis was conducted based on the open-source code by Parra and colleagues, which can be obtained at parralab.org/isc/ (for a detailed description, please see Parra et al., 2019). In short, covariance matrices at the viewer and channel levels were calculated within and between viewers from the preprocessed video data segments. ISC is defined as the ratio of the between-subjects covariance (i.e., the sum of covariance matrices of all pairs of viewers) and the within-subject covariance (i.e., the sum of covariance matrices of all viewers), normalized by a common scaling factor (see Parra et al., 2019). This ratio was estimated via generalized eigenvector decomposition with the constraint that the components be mutually uncorrelated. Unlike blind source separation procedures, such as PCA, which extract linearly independent components, ISC aims to fit a spatial filter by maximizing the contrast between specific data features, i.e., the between- and within-viewer covariances (cf. M. X. Cohen, 2022). In other words, the EEG-ISC can reveal shared neural signals in different viewers. The extracted eigenvectors, called maximally correlated components, represent linear combinations of sensors that reveal maximal correlation across viewers over time. Hence, these linear combinations of electrodes are common to all viewers. The EEG data for each viewer is then projected into this component space. For each correlated component, EEG-ISC is extracted, by averaging the Pearson correlation coefficient of the projected time-courses between all pairs of viewers in the respective group (e.g., S. S. Cohen & Parra, 2016). To obtain unbiased estimates, correlated components are calculated, for each participant group, using within- and between-subject covariance matrices averaged across all videos. In contrast to a voxel-by-voxel approach - as often used in fMRI - this approach allows detection of large-scale activity patterns, which otherwise could be occluded when using a sensor-by-sensor approach (e.g., Dmochowski et al., 2012). Based on inspection of the eigenvalue distribution (Supplementary Figure SM1) and the topographies of previous work (e.g., S. S. Cohen & Parra, 2016; Dmochowski et al., 2012; Imhof et al., 2020), we extracted three components. As in previous work, we calculated their forward models to visualize the spatial distribution of the correlated components (Figure 2a). The forward models represent the covariance between a component's signal and the signal at each sensor (Dmochowski et al., 2012; Haufe et al., 2014; Parra et al., 2005).

To analyze experimental effects, EEG-ISC was then extracted for each video and each participant, separately. We subsequently averaged the ISC values across strong and weak videos for each component and submitted them into three mixed repeated-measures analyses of variance (ANOVAs) with the within-subjects factor *Video Category* (strong vs. weak) and the between-subjects factor *Viewing Condition* (individual vs. group). Effect sizes were estimated by partial (η^2_p) and generalized (η^2_G) Eta squared. As the assumption of heteroscedasticity was not met for EEG-ISC of component C_3 ($Fs(1,39) > 7.04$, $ps < .02$; Levene's test), we conducted a robust repeated-measures ANOVA based on trimmed means. As statistical inferences drawn from both analyses did not differ, we report results of the parametric ANOVA for ease of comparison (Table 1). The non-parametric results are reported in the Supplementary (Table SR2). Subsequent post hoc *t*-tests were Holm-corrected to account for multiple comparisons. Effect sizes were calculated using Cohen's *d*.

In a second stream of robustness analyses, we assessed the spatial and temporal stability of the correlated components across viewing conditions and studies, that is, across EEG systems. For across-study comparisons we use data from an independent participant sample who viewed the same health messages while wearing high-density EEG (N = 32, 256-channel EEG, 1000 Hz sampling rate, band-pass filtered from .01 to 400 Hz; for details, see Imhof et al., 2020). For assessing spatial stability, we extracted the weight matrices for each sample and each correlated component at the sensor sites corresponding to the portable EEG (Figure SR1 & Table SR1). The resulting matrices were Fisher *z*-transformed and Pearson correlation coefficients were calculated to assess spatial correlation across viewing conditions and studies.

To assess temporal stability, we first calculated the time-resolved ISC for each video and each correlated component, using a 2 s sliding window with .25 s increments (Figure 3a). These ISC time courses were then used to assess the across-viewing and across-study stability. For each component and each video, we compared the Fisher *z*-transformed ISC time courses by means of Pearson correlation, resulting in three correlation values per video and per comparison (Figure 3b). These correlation coefficients were subsequently averaged across videos to report the across-study and across-group temporal stability for each component (Figure 3c).

Statistical analyses were conducted using MATLAB R2021b version 9.11.0.1809720 (The MathWorks Inc.), jasp version 0.17.1 (JASP Team, 2023) and R version 4.2.3 (R Core Team, 2022) with the R packages and "WRS2" (Mair & Wilcox, 2020) and "rstatix" (Kassambara, 2023)

Results

Perceived effectiveness of the videos

Perceived message effectiveness (PME) ratings were significantly correlated with those of the previous fMRI and EEG audiences (*rs* ≥ .96, *ps* ≤.001, independent data from Imhof et al., 2017, 2020). As in our previous work, the single-item PME measure was highly correlated with single-item scales measuring perceived argument strength and threatening content (*rs* ≥ .90, *ps* ≤ .001), supporting its use in examining message effectiveness in the current study.

Next, we assessed differences in PME ratings across viewing conditions using a mixed repeated measures ANOVA with the between subject factor *Viewing Condition* (individual vs. group viewing) and the within subject factor *Video Category* (strong vs. weak). The main effect of *Video Category* confirmed that strong messages were evaluated more effective (M_{Strong} = 5.85, *SE* = .37, M_{Weak} = 2.50, *SE* = .14; $F(1,18)$ = 71.65, p < .001, η_g^2 = .79, η_p^2 = .80). Furthermore, the main effect of *Viewing Condition* indicated that participants in the individual viewing condition evaluated the messages generally more effective compared to the group condition ($M_{\text{Individual}}$ = 4.43, *SE* = .46, M_{Group} = 3.94, *SE* = .40; $F(1,18)$ = 21.80, p < .001, η_g^2 = .07, η_p^2 = .55). The interaction of *Viewing Condition* with *Video Category* approached significance ($F(1,18)$ = 3.87, p = .065, η_g^2 = .01, η_p^2 = .18). Post hoc tests confirmed that strong messages were perceived more effective in both viewing conditions (*ts*(18) ≥ 7.68, Δ ≥ 3.15, *ps* < .001, Holm correction, Cohen's *ds* ≥ 3.43). In sum, PME ratings in the current audiences revealed high replicability and confirmed the distinction into strong and weak videos.

Spatially replicable correlated components using portable EEG

To be useful in translational settings, measures need to be consistent and reliable across settings. Thus, we determined whether low-density EEG could reveal the correlated components observed in previous research using high-density EEG. Figure 2a illustrates the topography of the three correlated components in the present study separately for the two viewing conditions. As can be seen, nearly the same topographies were observed across individual and group viewing conditions. The spatial correlations of the correlated components' topographies identified using portable EEG were very high across viewing conditions (rs > .96, ps < .001, , Bonferroni corrected). Comparing the topographies of the 24-channel portable EEG and data collected in previous research using high-density lab EEG (Imhof et al., 2020) revealed a remarkably consistent pattern for these correlated components (Fig. 2b). The correlated components' topographies also revealed a high spatial correlation with the topographies from high-density EEG with spatial correlations ranging from rs > .71 for C_2, to rs > .83 for C_3 and rs > .98 for C_1 (all ps < .0054, Bonferroni corrected, for details see Supplementary Table SR1 & Figure SR1). To assess the relation between spatial stability of the correlated components and sample size, we conducted an exploratory analysis, in which we randomly drew an increasing number of EEG data from the full sample (N = 41). As visualized in Figure SR2 (Supplementary Results), correlated component C_1 was identifiable - in our stimulus material and viewing setting - with data of at least three participants onwards. For components C_2 and C_3, component topographies appeared stable at about six participants onwards. In sum, the topographies brought out with low-density EEG show a close correspondence across viewing conditions and EEG systems.

Figure 2 here

Temporal stability of EEG-ISC across viewing conditions and EEG systems

To assess the temporal stability of the EEG-ISC, we calculated ISC resolved over time using a sliding window approach. Then, as shown in Figure 3a & 3b, Pearson correlations were computed to compare the time-resolved ISC for each correlated component across both, the individual and group viewing conditions in the current study, as well as the independent group from previous work using high-density lab EEG (Imhof et al., 2020).

Figure 3 here

As shown in Figure 3c, average across-sample correlations of the ISC time courses for each correlated component revealed remarkable replicability with average inter-correlations of up to $r_{Avg\text{-}C1}$ = .87 for C_1 (SD = .07, 95%-CI: .85 to .89) and medium to large average inter-sample correlations for correlated components C_2 and C_3 ($r_{Avg\text{-}C2}$ = .46, SD = .24, 95%-CI = .40 to .52; $r_{Avg\text{-}C3}$ = .33, SD = .19, 95%-CI = .28 to .38). Inter-sample correlations within the portable EEG data sets were even higher for C_2 and C_3 with $r_{GroupXIndividual\ C2}$ = .54 and $r_{GroupXIndividual\ C3}$ = .40. Overall, ISC over time as captured by the correlated components was reliable across viewing conditions and EEG systems.

Audience brain coupling across video categories and viewing conditions

Two test audiences were exposed to health messages while measuring portable EEG in two viewing conditions. As shown in Figure 4, the findings supported the two main hypothesis regarding differences in audience brain coupling as a function of health message effectiveness: First, replicating previous findings using high-density EEG, ISC was consistently enhanced during strong messages in the lab-like individual viewing condition. Second, the effect was extended to a context resembling a focus group. Lastly, this finding of enhanced audience brain coupling was highly consistent across viewers. Across both viewing conditions, the pattern was expressed in every audience member for C_1 and C_2, and in 40 (out of 41) for C_3. With respect to effects of viewing condition, there were less pronounced differences in ISC across viewing conditions for C_1 and C_3 with higher ISC in the individual compared to the group viewing condition.

Figure 4 here

To statistically confirm that strong messages prompted enhanced audience brain coupling, we submitted the level of ISC to mixed repeated measures ANOVAs including the within factor *Video Category* (strong vs. weak) and the between factor *Viewing Condition* (individual vs. group viewing) to show potential effects of the viewing setting.

Main effect Video Category: Enhanced audience brain coupling during strong messages

For all three correlated components, significant main effects of *Video Category* confirmed the expected enhancement of ISC during strong as compared to weak videos ($Fs(1,39) \geq 162.18$, $ps < .001$, $\eta_g^2 \geq .44$). For C_1 & C_3, the interaction of *Video Category* and *Viewing Condition* was not significant ($Fs(1,39) < 1.60$, $ps > .21$, *n.s.*; for details, see Table 1). For C_2, the main effect of *Video Category* was qualified by the significant interaction with *Viewing Condition* ($F(1,39) = 12.11$, $p = .001$, $\eta_g^2 = .04$). Post hoc-tests for C_2 confirmed that EEG-ISC was larger for strong videos in both viewing conditions ($ts(39) \geq 11.22$, $ps < .001$, Holm correction, Cohen's $ds \geq 1.87$).

Main effect Viewing Condition: Differences in brain coupling across groups

For correlated components C_1 and C_3, significant, albeit less pronounced main effects for *Viewing Condition* showed that ISC in the individual viewing condition was larger compared to the group viewing condition ($Fs(1,39) \geq 5.39$, $ps \leq .026$, $\eta_g^2 \geq .10$). For C_2, the main effect of *Viewing Condition* was not significant ($F(1,39) = 1.30$, $p = .26$, *n.s.*). Post hoc tests following up the significant two-way interaction for C_2 showed that, during strong videos, ISC was larger in the group setting compared to individual viewing ($t(39) = 2.35$, $p < .05$, Holm correction, Cohen's $d = .74$, Figure SR3 in the Supplementary Results). This effect was not seen for weak videos ($t(39) = .24$, $p = .81$, *n.s.*).

Table 1 here

Discussion

Measuring brain responses offers insights into how messages affect recipients and can thus contribute to the development of more effective health campaigns (Falk, 2010). It is critical, however, that findings obtained in optimized conditions, such as the shielded chambers of EEG labs or dedicated fMRI scanners, can be replicated in real-world settings (cf. Nastase et al., 2020; Shamay-Tsoory & Mendelsohn, 2019). The present study addressed two challenges for neural measures in the context of health communication. First, we show that ISC is feasible and remains sensitive with low-density portable EEG. Two main findings support this assumption: The current study replicated reliably the correlated components obtained using high-density 256-channel EEG in a lab setting. Furthermore, ISC captured by the components was sensitive to the experimental manipulation, replicating the finding of enhanced EEG-ISC for strong health messages (Imhof et al., 2020). Second, we show that assessing neural data during health message reception is feasible in groups, which is more efficient and opens new avenues for audience research. This is supported by the equal results obtained when six participants were measured simultaneously compared to the traditional, one-person-at-a-time individual viewing setting. Overall, these results support a translational perspective on the use of neuroscience measures in health message development.

EEG research has been on the forefront for collecting neural data in non-laboratory settings. For instance, portable, low-density EEG has been successfully used to replicate laboratory EEG findings during attention and engagement (e.g., Bleichner & Debener, 2017; Debener et al., 2015; Holtze et al., 2022; Krigolson et al., 2021; Poulsen et al., 2017). Here, we assessed whether EEG-ISC can be measured reliably with portable devices and in non-laboratory settings. Conceptually, EEG-ISC relies on a spatial filtering approach in which linear combinations of scalp sensors are sought that maximize the correlation across the audience (cf. Parra et al., 2019). Thus, to obtain correlated components reliably, scalp sensor density needs to be sufficient. The 24-channel montage used here has inherently less head coverage and a lower spatial resolution of ~6 cm inter-sensor distances, especially compared to the previously used 256-channel montage with ~2 cm distances (Imhof et al., 2020). Nevertheless, spatial correlations ranged from *r* = .71 to .97 when comparing the correlated components' topographies for portable EEG and high-density EEG. Interestingly, the order of the correlated components – based on their amount of captured ISC – differed in part compared to our previous work (see Figure 2; Imhof et al., 2020). However, even with reduced spatial coverage and resolution, the main correlated components were retrieved in the signal and resembled those previously seen in work with audio-visual stimuli in general (S. S. Cohen & Parra, 2016; Dmochowski et al., 2012; Poulsen et al., 2017) and video health messages in particular (Imhof et al., 2020).

In addition to replicating the topographies, testing the sensitivity of the correlated components' ISC to message strength is critical; after all, the premise of using neuroscience for message testing is that it is sensitive to variations in relevant message characteristics. Thus, the second key finding is that even with low-density portable EEG, brain coupling was robustly enhanced during the reception of strong messages. In previous work, we linked ISC of these components to fMRI-BOLD signal changes (Imhof et al., 2020). Relations were seen not only within primary sensory regions, but also within the posterior cingulate cortex (C_2), the insula and precuneus (C_2 and C_3) as well as the anterior cingulate and dorsomedial prefrontal cortex (C_3) - brain regions commonly linked to personal relevance, affect and attentional processes more broadly (Etkin et al., 2011; Murray et al., 2012; Qin & Northoff, 2011; Raichle, 2015; Schmitz & Johnson, 2007; Shackman et al., 2011). Within the context of naturalistic health message processing, replicating enhanced brain coupling to strong messages demonstrates that ISC with portable EEG is robust and sensitive to message strength, underscoring its potential as a neural marker of effective messaging. Future research should extend these promising findings to other public health topics.

Developing robust and efficient message evaluation protocols has been an important topic in health communication. For instance, a recent protocol relying on survey measures suggested that an audience of around 25 individuals is sufficient to select the most promising health messages from a larger pool (Kim & Cappella, 2019). From a translational perspective, it is thus encouraging that neural measures are obtainable with similar sample sizes. However, the need to collect data in a serial, one-person-at-a-time manner considerably prolongs the duration of data collection and limits its potential. To connect to social scientific methods, one could envision “neural focus groups” in which brain measures collected in the audience may aid in selecting health messages (Falk, 2010). Previous research has shown that group EEG is feasible in settings ranging from the classroom (e.g., Dikker et al., 2017; Poulsen et al., 2017), to game playing and cooperation (e.g., Astolfi et al., 2010; Reinero et al., 2020), to musicians performing together (e.g., Babiloni et al., 2012; Müller & Lindenberger, 2023). However, a prerequisite for using group recordings in message testing is that neuroscientific measures in groups can reproduce individually obtained component topographies and sensitivity to message strength. In this study, the topographies in the group setting closely replicated the individual condition and showed high spatial and temporal stability. Even more importantly, the correlated components showed increased brain coupling for strong messages, with large effect sizes in both viewing settings. While not optimized for this type of analysis, exploratory analyses showed that ISC was positively related to self-reported PME, as indicated by robust rank correlation coefficients for EEG-ISC of components C_1 to C_3 (Spearman's ρs = .63 to .76 all ps < .0038, see Supplementary Results Table SR 3) in both viewing conditions. However, health messages in this study were pre-selected from the upper and lower end of the PME distribution from Imhof et al. (2017). Thus, while we anticipate that neural measures may aid in brain-based message selection, future work with messages that cover the full range of message strength is needed to assess the relation of ISC and message strength. Rapid progress in technology might further pave the way for application by making EEG systems unobtrusive and easier to apply, such as around-the-ear devices (Bleichner & Debener, 2017; Holtze et al., 2022). Overall, the current results suggest that neuroscientific measures might progress along the translational continuum to a stage where message evaluation protocols are feasible.

Health messages are seen individually or in the company of others, and this co-viewing may alter viewing experience. For example, social influences can shape message effects on individuals, and several mediators and moderators, such as group identity, or audience reactions have been identified (Tal-Or, 2021). In the current work, differential ISC effects between strong and weak messages were similarly consistent and comparable in effect size for both, co-viewing in a group and individual viewing (see Table 1). In addition, albeit with lower effect sizes compared to message strength, EEG-ISC was also modulated by viewing conditions. ISC captured by the correlated component C_1 was larger in the individual than in the group viewing setting. Based on our previous observation that EEG-ISC of this component may primarily reflect sensory processing (Imhof et al., 2020), lower ISC in the group setting might be related to distraction or divided attention. Interestingly, EEG-ISC of components C_2 and C_3, which have been conceptually related to personal relevance, affect, and attention regulation (cf. Imhof et al., 2020), were differentially modulated by viewing condition. Specifically, ISC of component C_2 was larger during group than individual viewing. It is a common finding in media psychology that co-viewing can enhance audience response, e.g., during public viewing of soccer matches or friends watching shows together (Tal-Or, 2021). Similarly, a group setting may have effects on the reception of health messages due to shared attention and collective emotions, which in turn, might influence attitude change (Tal-Or, 2016). However, ISC of component C_3 was larger in the individual than group viewing condition demonstrating more nuanced relationships between message processing and viewing condition. One may speculate that viewing the health messages individually or in a group context may invoke shifts between intrinsically and extrinsically oriented neural processing (cf. Golland et al., 2007; Yeshurun et al., 2021), leading to differential EEG-ISC effects seen in the distinct correlated component. This hypothesis could be examined in future research using functional imaging to consider the relation between neural effects of health message reception and task effects, specifically guiding intrinsic and extrinsic processing modes. Furthermore, as a caveat, one needs to consider that increases in ISC may also be artificially induced, for instance by shared noise (e.g., Burgess, 2013). Overall, portable EEG appears suitable to both, individual and group measurements, and thus especially useful for exploring co-viewing effects on health message processing due to its accessibility. For example, real-world conditions of health message reception can be mimicked by comparing individual viewing to co-viewing with friends and peers (cf. Baek & Parkinson, 2022).

A limitation of the present study is that previous findings on the association between health message processing and change in drinking behavior were not replicated. Specifically, we previously observed that ISC of components C_2 and C_3 was a predictor of reductions in risky drinking, explaining variance going beyond self-report measures (Imhof et al., 2020). Such findings motivate the use of self-report and brain measures in concert, and thus, are of particular importance. A critical difference between the present and previous research regards the variability of drinking behavior, which was considerably reduced in the current sample. This change in drinking behavior may be related to the unique circumstances invoked by the Covid-19 pandemic which - among many other changes - affected college student drinking behavior. For instance, Covid-19-related increases in drinking frequency went along with decreases in drinking amounts, heavy drinking, as well as reduced opportunities for social drinking (Jackson et al., 2021). It thus seems possible that these changes contributed to the reduced variability of drinking behavior in this study, which may have hindered the replication of previously seen effects. Overall, it seems important to confirm our initial observations in future studies using larger sample sizes.

Neuroscientific measures provide a valuable tool for message testing in health communication, adding significant value beyond self-report measures (Falk et al., 2010; Weber et al., 2018). A particularly valuable line in communication neuroscience is the brain-as-predictor approach in which neural activity recorded during health message processing is linked to behavior change (Berkman & Falk, 2013; Falk et al., 2010; Falk et al., 2015). Developing effective health campaigns requires messages that achieve their aims within the target audience. The present findings suggest that focus groups in which health messages are screened in small target groups, can be extended to a neural focus group approach. Previous research showed that EEG-ISC predicted behavioral measures more reliably in large audiences, that is, the population, than in the sample where EEG was recorded (Dmochowski et al., 2014). Thus, the neural signal may not only provide insights into the processes underlying message reception but also represent a reliable predictor of message effectiveness in target audiences. Prospectively, neural measures obtained from relatively small samples could complement the common practice of extensive audience research using large samples, a concept known as neuroforecasting (see Genevsky & Yoon, 2022 for a review).

Conclusion

Translating neuroscientific research to real-world applications faces challenges concerning costs, time, and feasibility of data collection. The present study served as a proof-of-principle that some of the challenges can be met. We demonstrated that the EEG-ISC approach is feasible when using data from groups exposed to health messages. Importantly, portable low-density devices replicated findings of increased brain coupling to strong health messages in groups of six participants. These findings support the view that combining the ISC approach with cost-effective - and thus scalable - group EEG offers potential beyond the laboratory. Enriching message development with insights from neuroscientific measures may help to make messages more effective. Considering that health messages reach millions, even small improvements may lead to consequential differences.

Author information

Funding

This work was supported by the Messmer Foundation [grant to MI], the Centre for the Advanced Study of Collective Behaviour, funded by the Deutsche Forschungsgemeinschaft (DFG, German Research Foundation) under Germany's Excellence Strategy [EXC2117-422037984 granted to HS] and the DFG grant [FOR 2374, http://gepris.dfg.de/gepris/projekt/273711585) granted to BR and HS].

Acknowledgements

We thank the Parra Lab for sharing their code and expertise. We thank Ursula Kirmse and Tobias Flaisch for valuable discussions. We thank Katharina Natter for help with project administration and data collection. We thank Kassandra Huitron, Daniel Madel, Pia Kohler, and Sarah Tischinger for help with data collection.

Competing interests

The authors declare no competing interests.

CRediT author statement

Martin A. Imhof: Conceptualization, Methodology, Software, Formal analysis, Investigation , Writing - Original Draft, Review & Editing, Visualization, Supervision, Project administration, Funding acquisition; **Karl-Philipp Flösch:** Methodology, Software, Formal analysis, Writing - Original Draft, Review & Editing; **Ralf Schmälzle:** Conceptualization, Methodology, Visualization, Writing - Original Draft, Review & Editing; **Britta Renne**r: Writing - Review & Editing, Funding acquisition; **Harald T. Schupp:** Conceptualization, Writing - Original Draft, Review & Editing, Funding acquisition.

Data availability

Data to reproduce the main findings visualized in Figure 2 as well as intermediary data and accompanying component models are available for download at https://osf.io/je874/. The full data supporting the findings of this study is available from the corresponding author upon reasonable request. Due to copyright restrictions and data privacy, the stimulus material as well as the raw data cannot be made publicly available. Detailed stimulus descriptions are available in previous work (doi.org/10.1093/scan/nsx044).

Code availability

The code that was used for the analyses is in part based on the MATLAB code of the Parra Lab, which has been retrieved from http://www.parralab.org/isc/ . The full code to reproduce the results is available from the corresponding author upon request.

References

Astolfi, L., Cincotti, F., Mattia, D. et al. (2010). Simultaneous estimation of cortical activity during social interactions by using EEG hyperscannings. In *2010 Annual International Conference of the IEEE Engineering in Medicine and Biology.* IEEE. https://doi.org/10.1109/iembs.2010.5626555

Babiloni, C., Buffo, P., Vecchio, F. et al. (2012). Brains "in concert": Frontal oscillatory alpha rhythms and empathy in professional musicians. *NeuroImage*, *60*(1), 105–116. https://doi.org/10.1016/j.neuroimage.2011.12.008

Babor, T. F., Higgins-Biddle, J. C., Saunders, J. B., & Monteiro, M. G. (2001). *AUDIT: The Alcohol Use Disorders Identification Test*. Guidelines for Use in Primary Care. Geneva, Switzerland. World Health Organization. http://apps.who.int/iris/bitstream/10665/67205/1/WHO_MSD_MSB_01.6a.pdf

Baek, E. C., & Parkinson, C. (2022). Shared understanding and social connection: Integrating approaches from social psychology, social network analysis, and neuroscience. *Social and Personality Psychology Compass*, *16*(11), e12710. https://doi.org/10.1111/spc3.12710

Barnett, S. B., & Cerf, M. (2017). A Ticket for Your Thoughts: Method for Predicting Content Recall and Sales Using Neural Similarity of Moviegoers. *Journal of Consumer Research*, 160-181. https://doi.org/10.1093/jcr/ucw083

Berkman, E. T., & Falk, E. B. (2013). Beyond Brain Mapping: Using Neural Measures to Predict Real-World Outcomes. *Current Directions in Psychological Science*, *22*(1), 45–50. https://doi.org/10.1177/0963721412469394

Berns, G. S., & Moore, S. E. (2012). A neural predictor of cultural popularity. *Journal of Consumer Psychology*, *22*(1), 154–160. https://doi.org/10.1016/j.jcps.2011.05.001

Bleichner, M. G., & Debener, S. (2017). Concealed, Unobtrusive Ear-Centered EEG Acquisition: Ceegrids for Transparent EEG. *Frontiers in Human Neuroscience*, *11*, 163. https://doi.org/10.3389/fnhum.2017.00163

Burgess, A. P. (2013). On the interpretation of synchronization in EEG hyperscanning studies: A cautionary note. *Frontiers in Human Neuroscience*, *7*, 881. https://doi.org/10.3389/fnhum.2013.00881

Cochrane, A. L. (1972). *Effectiveness and efficiency: Random reflections on health services*. Cohe. *The Rock Carling Fellowship*. Nuffield Trust.

Cohen, M. X. (2022). A tutorial on generalized eigendecomposition for denoising, contrast enhancement, and dimension reduction in multichannel electrophysiology. *NeuroImage*, *247*, 118809. https://doi.org/10.1016/j.neuroimage.2021.118809

Cohen, S. S., & Parra, L. C. (2016). Memorable Audiovisual Narratives Synchronize Sensory and Supramodal Neural Responses. *ENeuro*, *3*(6). https://doi.org/10.1523/ENEURO.0203-16.2016

Debener, S., Emkes, R., Vos, M. de, & Bleichner, M. (2015). Unobtrusive ambulatory EEG using a smartphone and flexible printed electrodes around the ear. *Scientific Reports*, *5*, 16743. https://doi.org/10.1038/srep16743

Dikker, S., Wan, L., Davidesco, I. et al. (2017). Brain-to-Brain Synchrony Tracks Real-World Dynamic Group Interactions in the Classroom. *Current Biology*, *27*(9), 1375–1380. https://doi.org/10.1016/j.cub.2017.04.002

Dmochowski, J. P., Bezdek, M. A., Abelson, B. P., Johnson, J. S., Schumacher, E. H., & Parra, L. C. (2014). Audience preferences are predicted by temporal reliability of neural processing. *Nature Communications*, *5*, 4567. https://doi.org/10.1038/ncomms5567

Dmochowski, J. P., Sajda, P., Dias, J., & Parra, L. C. (2012). Correlated components of ongoing EEG point to emotionally laden attention - a possible marker of engagement? *Frontiers in Human Neuroscience*, *6*, 112. https://doi.org/10.3389/fnhum.2012.00112

Drolet, B. C., & Lorenzi, N. M. (2011). Translational research: Understanding the continuum from bench to bedside. *Translational Research : The Journal of Laboratory and Clinical Medicine*, *157*(1), 1–5. https://doi.org/10.1016/j.trsl.2010.10.002

Etkin, A., Egner, T., & Kalisch, R. (2011). Emotional processing in anterior cingulate and medial prefrontal cortex. *Trends in Cognitive Sciences*, *15*(2), 85–93. https://doi.org/10.1016/j.tics.2010.11.004

Falk, E. B. (2010). Communication neuroscience as a tool for health psychologists. *Health Psychology*, *29*(4), 355–357. https://doi.org/10.1037/a0020427

Falk, E. B., Berkman, E. T., Mann, T., Harrison, B., & Lieberman, M. D. (2010). Predicting persuasion-induced behavior change from the brain. *The Journal of Neuroscience*, *30*(25), 8421–8424. https://doi.org/10.1523/JNEUROSCI.0063-10.2010

Falk, E. B., Cascio, C. N., & Coronel, J. C. (2015). Neural Prediction of Communication-Relevant Outcomes. *Communication Methods and Measures*, *9*(1-2), 30–54. https://doi.org/10.1080/19312458.2014.999750

Faul, F., Erdfelder, E., Lang, A.-G., & Buchner, A. (2007). G*power 3: A flexible statistical power analysis program for the social, behavioral, and biomedical sciences. *Behavior Research Methods*, *39*(2), 175–191. https://doi.org/10.3758/BF03193146
Genevsky, A., & Yoon, C. (2022). Neural basis of consumer decision making and neuroforecasting. In L. R. Kahle, T. M. Lowrey, & J. Huber (Eds.), *APA handbook of consumer psychology* (pp. 621–635). American Psychological Association. https://doi.org/10.1037/0000262-027
Golland, Y., Bentin, S., Gelbard, H. et al. (2007). Extrinsic and intrinsic systems in the posterior cortex of the human brain revealed during natural sensory stimulation. *Cerebral Cortex (New York, N.Y. : 1991)*, *17*(4), 766–777. https://doi.org/10.1093/cercor/bhk030
Hasson, U., Ghazanfar, A. A., Galantucci, B., Garrod, S., & Keysers, C. (2012). Brain-to-brain coupling: A mechanism for creating and sharing a social world. *Trends in Cognitive Sciences*, *16*(2), 114–121. https://doi.org/10.1016/j.tics.2011.12.007
Hasson, U., Malach, R., & Heeger, D. J. (2010). Reliability of cortical activity during natural stimulation. *Trends in Cognitive Sciences*, *14*(1), 40–48. https://doi.org/10.1016/j.tics.2009.10.011
Haufe, S., Meinecke, F., Görgen, K. et al. (2014). On the interpretation of weight vectors of linear models in multivariate neuroimaging. *NeuroImage*, *87*, 96–110. https://doi.org/10.1016/j.neuroimage.2013.10.067
Haynes, B. (1999). Can it work? Does it work? Is it worth it? The testing of healthcare interventions is evolving. *BMJ (Clinical Research Ed.)*, *319*(7211), 652–653. https://doi.org/10.1136/bmj.319.7211.652
Holtze, B., Rosenkranz, M., Jaeger, M., Debener, S., & Mirkovic, B. (2022). Ear-EEG Measures of Auditory Attention to Continuous Speech. *Frontiers in Neuroscience*, *16*, 869426. https://doi.org/10.3389/fnins.2022.869426
Imhof, M. A., Schmälzle, R., Renner, B., & Schupp, H. T. (2017). How real-life health messages engage our brains: Shared processing of effective anti-alcohol videos. *Social Cognitive and Affective Neuroscience*, *12*(7), 1188–1196. https://doi.org/10.1093/scan/nsx044
Imhof, M. A., Schmälzle, R., Renner, B., & Schupp, H. T. (2020). Strong health messages increase audience brain coupling. *NeuroImage*, 116527. https://doi.org/10.1016/j.neuroimage.2020.116527
Jääskeläinen, I. P., Sams, M., Glerean, E., & Ahveninen, J. (2021). Movies and narratives as naturalistic stimuli in neuroimaging. *NeuroImage*, *224*, 117445. https://doi.org/10.1016/j.neuroimage.2020.117445
Jackson, K. M., Merrill, J. E., Stevens, A. K., Hayes, K. L., & White, H. R. (2021). Changes in Alcohol Use and Drinking Context due to the COVID-19 Pandemic: A Multimethod Study of College Student Drinkers. *Alcoholism, Clinical and Experimental Research*, *45*(4), 752–764. https://doi.org/10.1111/acer.14574
JASP Team. (2023). *JASP (Version 0.17.1)* [Computer software]. https://jasp-stats.org/.
Kassambara, A. (2023). *rstatix: Pipe-Friendly Framework for Basic Statistical Tests* (Version 0.7.2) [Computer software]. https://CRAN.R-project.org/package=rstatix.
Kaye, S.-A., White, M. J., & Lewis, I. (2016). The use of neurocognitive methods in assessing health communication messages: A systematic review. *Journal of Health Psychology.* Advance online publication. https://doi.org/10.1177/1359105316630138
Kim, M., & Cappella, J. N. (2019). An Efficient Message Evaluation Protocol: Two Empirical Analyses on Positional Effects and Optimal Sample Size. *Journal of Health Communication*, *24*(10), 761–769. https://doi.org/10.1080/10810730.2019.1668090
Krigolson, O. E., Hammerstrom, M. R., Abimbola, W. et al. (2021). Using Muse: Rapid Mobile Assessment of Brain Performance. *Frontiers in Neuroscience*, *15*, 634147. https://doi.org/10.3389/fnins.2021.634147
Madsen, J., & Parra, L. C. (2022). Cognitive processing of a common stimulus synchronizes brains, hearts, and eyes. *PNAS Nexus*, *1*(1), pgac020. https://doi.org/10.1093/pnasnexus/pgac020
Mair, P., & Wilcox, R. (2020). Robust statistical methods in R using the WRS2 package. *Behavior Research Methods*, *52*(2), 464–488. https://doi.org/10.3758/s13428-019-01246-w
Merton, R. K., & Kendall, P. L. (1946). The Focused Interview. *American Journal of Sociology*, *51*(6), 541–557. https://doi.org/10.1086/219886
Müller, V., & Lindenberger, U. (2023). Intra- and interbrain synchrony and hyperbrain network dynamics of a guitarist quartet and its audience during a concert. *Annals of the New York Academy of Sciences*, *1523*(1), 74–90. https://doi.org/10.1111/nyas.14987
Murray, R. J., Schaer, M., & Debbané, M. (2012). Degrees of separation: A quantitative neuroimaging meta-analysis investigating self-specificity and shared neural activation between self- and other-reflection. *Neuroscience and Biobehavioral Reviews*, *36*(3), 1043–1059. https://doi.org/10.1016/j.neubiorev.2011.12.013

Nastase, S. A., Goldstein, A., & Hasson, U. (2020). Keep it real: Rethinking the primacy of experimental control in cognitive neuroscience. *NeuroImage*, *222*, 117254. https://doi.org/10.1016/j.neuroimage.2020.117254

Parra, L. C., Haufe, S., & Dmochowski, J. P. (2019). Correlated Components Analysis - Extracting Reliable Dimensions in Multivariate Data. *Neurons, Behavior, Data Analysis and Theory*. https://doi.org/10.51628/001c.7125

Parra, L. C., Spence, C. D., Gerson, A. D., & Sajda, P. (2005). Recipes for the linear analysis of EEG. *NeuroImage*, *28*(2), 326–341. https://doi.org/10.1016/j.neuroimage.2005.05.032

Poulsen, A. T., Kamronn, S., Dmochowski, J., Parra, L. C., & Hansen, L. K. (2017). EEG in the classroom: Synchronised neural recordings during video presentation. *Scientific Reports*, *7*, 43916. https://doi.org/10.1038/srep43916

Qin, P., & Northoff, G. (2011). How is our self related to midline regions and the default-mode network? *NeuroImage*, *57*(3), 1221–1233. https://doi.org/10.1016/j.neuroimage.2011.05.028

R Core Team. (2022). *R: A Language and Environment for Statistical Computing* [Computer software]. R Foundation for Statistical Computing. Vienna, Austria. https://www.R-project.org.

Raichle, M. E. (2015). The brain's default mode network. *Annual Review of Neuroscience*, *38*, 433–447. https://doi.org/10.1146/annurev-neuro-071013-014030

Reinero, D. A., Dikker, S., & van Bavel, J. J. (2020). Inter-brain synchrony in teams predicts collective performance. *Social Cognitive and Affective Neuroscience*, Volume 16, Issue 1-2, January-February 2021, 43–57. https://doi.org/10.31234/osf.io/k2ft6

Rice, R. E., & Atkin, C. K. (Eds.). (2013). *Public communication campaigns* (4. ed.). SAGE.

Rumpf, H.-J., Hapke, U., Meyer, C., & John, U. (2002). Screening for alcohol use disorders and at-risk drinking in the general population: Psychometric performance of three questionnaires. *Alcohol and Alcoholism*, *37*(3), 261–268. https://doi.org/10.1093/alcalc/37.3.261

Schmälzle, R. (2022). Theory and Method for Studying How Media Messages Prompt Shared Brain Responses Along the Sensation-to-Cognition Continuum. *Communication Theory*, Article qtac009. Advance online publication. https://doi.org/10.1093/ct/qtac009

Schmälzle, R., Cooper, N., O'Donnell, M. B. et al. (2020). The Effectiveness of Online Messages for Promoting Smoking Cessation Resources: Predicting Nationwide Campaign Effects From Neural Responses in the EX Campaign. *Frontiers in Human Neuroscience*, *14*, 565772. https://doi.org/10.3389/fnhum.2020.565772

Schmälzle, R., Häcker, F. E. K., Honey, C. J., & Hasson, U. (2015). Engaged listeners: Shared neural processing of powerful political speeches. *Social Cognitive and Affective Neuroscience*, *10*(8), 1137–1143. https://doi.org/10.1093/scan/nsu168

Schmälzle, R., Häcker, F. E., Renner, B., Honey, C. J., & Schupp, H. T. (2013). Neural Correlates of Risk Perception during Real-Life Risk Communication. *The Journal of Neuroscience*, *33*(25), 10340–10347. https://doi.org/10.1523/JNEUROSCI.5323-12.2013

Schmitz, T. W., & Johnson, S. C. (2007). Relevance to self: A brief review and framework of neural systems underlying appraisal. *Neuroscience and Biobehavioral Reviews*, *31*(4), 585–596. https://doi.org/10.1016/j.neubiorev.2006.12.003

Shackman, A. J., Salomons, T. V., Slagter, H. A., Fox, A. S., Winter, J. J., & Davidson, R. J. (2011). The integration of negative affect, pain and cognitive control in the cingulate cortex. *Nature Reviews. Neuroscience*, *12*(3), 154–167. https://doi.org/10.1038/nrn2994

Shamay-Tsoory, S. G., & Mendelsohn, A. (2019). Real-Life Neuroscience: An Ecological Approach to Brain and Behavior Research. *Perspectives on Psychological Science*, *14*(5), 841–859. https://doi.org/10.1177/1745691619856350

Tal-Or, N. (2016). How Co-Viewing Affects Attitudes: The Mediating Roles of Transportation and Identification. *Media Psychology*, *19*(3), 381–405. https://doi.org/10.1080/15213269.2015.1082918

Tal-Or, N. (2021). The Effects of Co-Viewers on the Viewing Experience. *Communication Theory*, *31*(3), 316–335. https://doi.org/10.1093/ct/qtz012

Wakefield, M. A., Loken, B., & Hornik, R. C. (2010). Use of mass media campaigns to change health behaviour. *The Lancet*, *376*(9748), 1261–1271. https://doi.org/10.1016/S0140-6736(10)60809-4

Weber, R., Fisher, J. T., Hopp, F. R., & Lonergan, C. (2018). Taking messages into the magnet: Method–theory synergy in communication neuroscience. *Communication Monographs*, *85*(1), 81–102. https://doi.org/10.1080/03637751.2017.1395059

Weber, R., Huskey, R., Mangus, J. M., Westcott Baker, A., & Turner, B. O. (2014). Neural Predictors of Message Effectiveness during Counterarguing in Antidrug Campaigns. *Communication Monographs*, *82*(1), 4–30. https://doi.org/10.1080/03637751.2014.971414

Wolf, S. (1974). Editorial: The real gap between bench and bedside. *The New England Journal of Medicine*, *290*(14), 802–803. https://doi.org/10.1056/NEJM197404042901411
Yeshurun, Y., Nguyen, M., & Hasson, U. (2021). The default mode network: Where the idiosyncratic self meets the shared social world. *Nature Reviews. Neuroscience.* Advance online publication. https://doi.org/10.1038/s41583-020-00420-w
Zink, R., Hunyadi, B., van Huffel, S., & Vos, M. de (2016). Mobile EEG on the bike: Disentangling attentional and physical contributions to auditory attention tasks. *Journal of Neural Engineering*, *13*(4), 46017. https://doi.org/10.1088/1741-2560/13/4/046017

Figure Legends

Figure 1 | Experimental setting and recording setup. a) Participants viewed the video health messages while sitting in a semicircle. Groups of six participants sat next to each other while watching the video health messages. In the "Individual Viewing" setting, one participant watched the videos in the same room setup. Recording laptops received the wirelessly transmitted EEG signal. The video health messages were projected onto the wall. Sound was delivered via speakers located in the front beneath the projection. b) Analysis scheme: Correlated components and ISC were extracted separately for each viewing condition and compared in a 2 x 2 mixed repeated measures design. c) Portable EEG amplifier, 24-channel gel-based sensor net and sensor positions (image used by permission of mbt: mbraintrain. The content in this lower left panel is not covered by the terms of the Creative Commons license of this publication. For permission to reuse, please contact mbt: mbraintrain).

Figure 2 | Maximally Correlated EEG Components captured using low-density portable EEG during the viewing of alcohol prevention videos. a) Topographical maps visualize the scalp projections, i.e., the forward models of the correlated components C_1 to C_3 obtained using portable EEG. Scalp projection magnitude represents the strength to which each sensor contributes to a component (blue to yellow - arbitrary units, polarity of projections normalized). b) Topographical maps obtained in previous work with high-density lab EEG reveal inter-study stability (Data from Imhof et al. (2020); for illustrative purposes components are re-ordered to resemble the order of the current work).

Figure 3 | Stability of EEG-ISC Inter-Sample Correlations. a) Exemplary ISC over Time is shown for Video 5. A 2 s-sliding window is used to calculate ISC over Time separately for each Correlated Component and each sample (Individual Viewing: $N = 21$, Group Viewing: $N = 20$ & Individual Lab EEG: $N = 32$). b) Correlation matrices show for each video the Pearson correlation coefficients across ISC time courses of all combinations of samples. c) Left: Box plots illustrate distribution and average inter-sample correlations, center lines represent sample median, hinges represent 25^{th} and 75^{th} percentiles. Right: Average inter-sample correlations across samples and components.

Figure 4 | Maximally *C*orrelated EEG *C*omponents reveal differences in ISC for low-density portable EEG data during the viewing of alcohol prevention videos – irrespective of *V*iewing *C*ondition. Box plots show average EEG-ISC for each correlated component, separated by the message categories Strong (red) and Weak (blue). Post hoc tests are visualized for the factor Video Category. Connecting lines visualize paired measures for all participants. Participants exhibiting a reversed pattern of results (ISC_{Weak} > ISC_{Strong}) are colored red. Colored dots within box represent the mean, center line represents the sample median, hinges represent the 25th and 75th percentiles, outliers are marked by a red cross. Asterisks indicate significance of two-sided, paired samples t-tests, *** = $p < .001$, Holm correction.

Figure 1

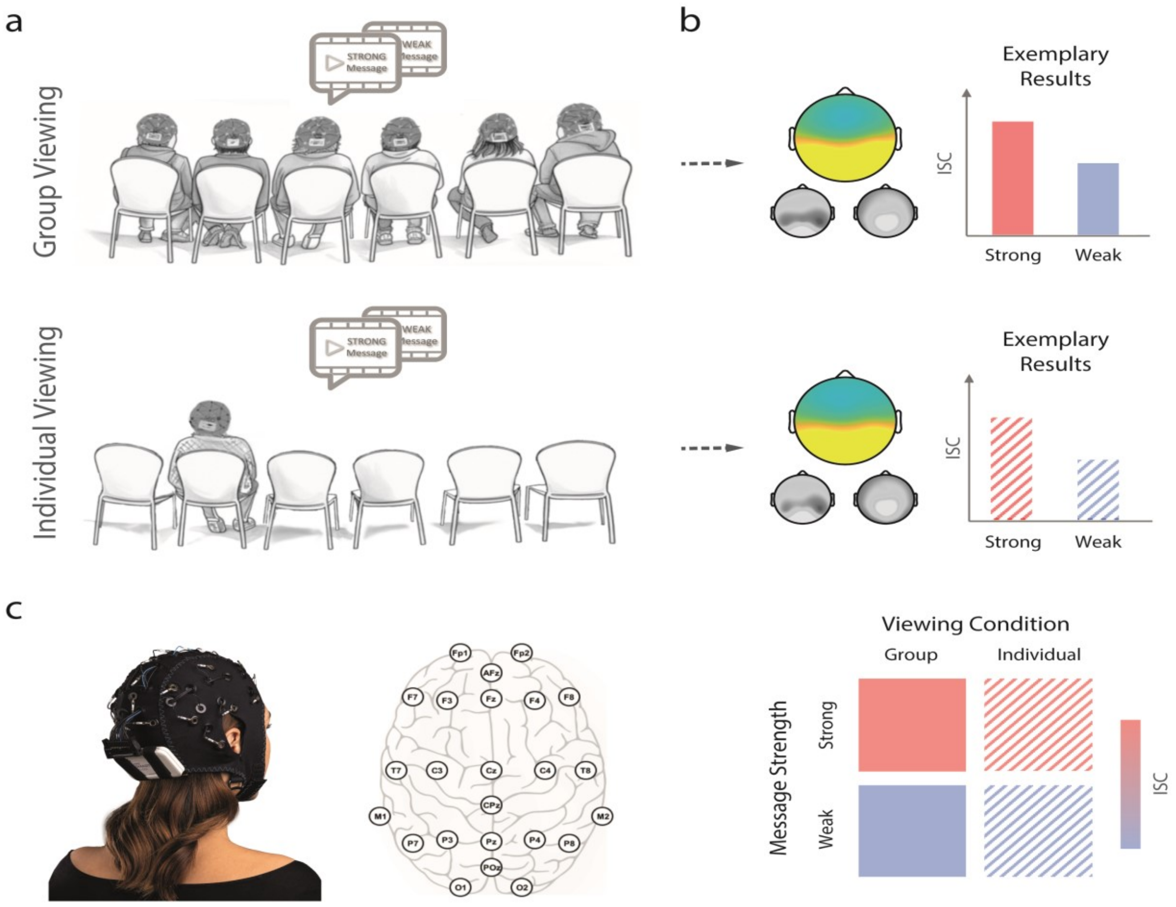
a
b
c
Group Viewing
Individual Viewing
STRONG Message
WEAK Message
Exemplary Results
ISC
Strong
Weak
Viewing Condition
Group
Individual
Message Strength
Strong
Weak
ISC

Figure 2

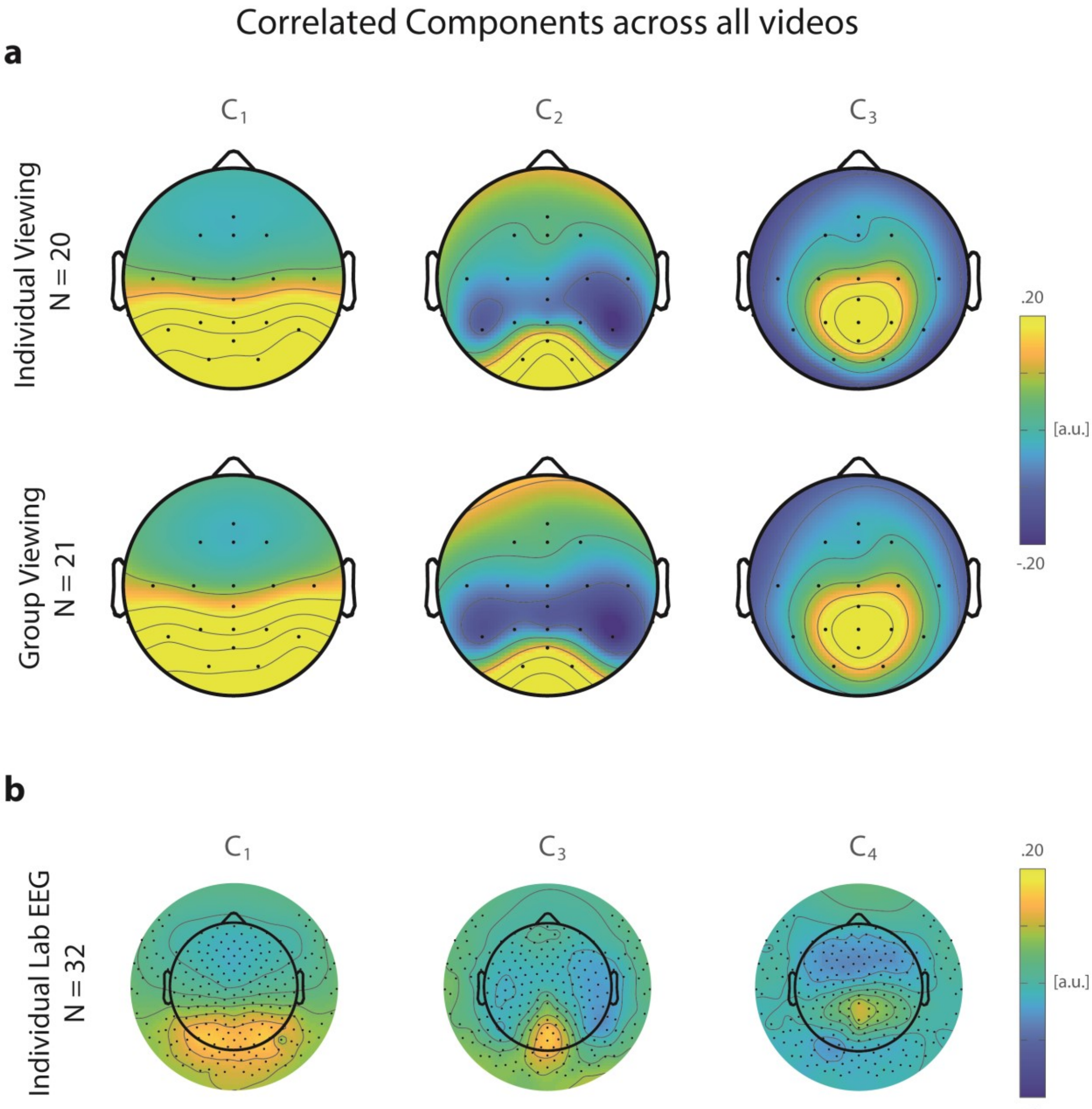
Correlated Components across all videos
a
C_1
C_2
C_3
Individual Viewing
N = 20
Group Viewing
N = 21
.20
[a.u.]
-.20
b
C_1
C_3
C_4
Individual Lab EEG
N = 32
.20
[a.u.]
-.20

Figure 3

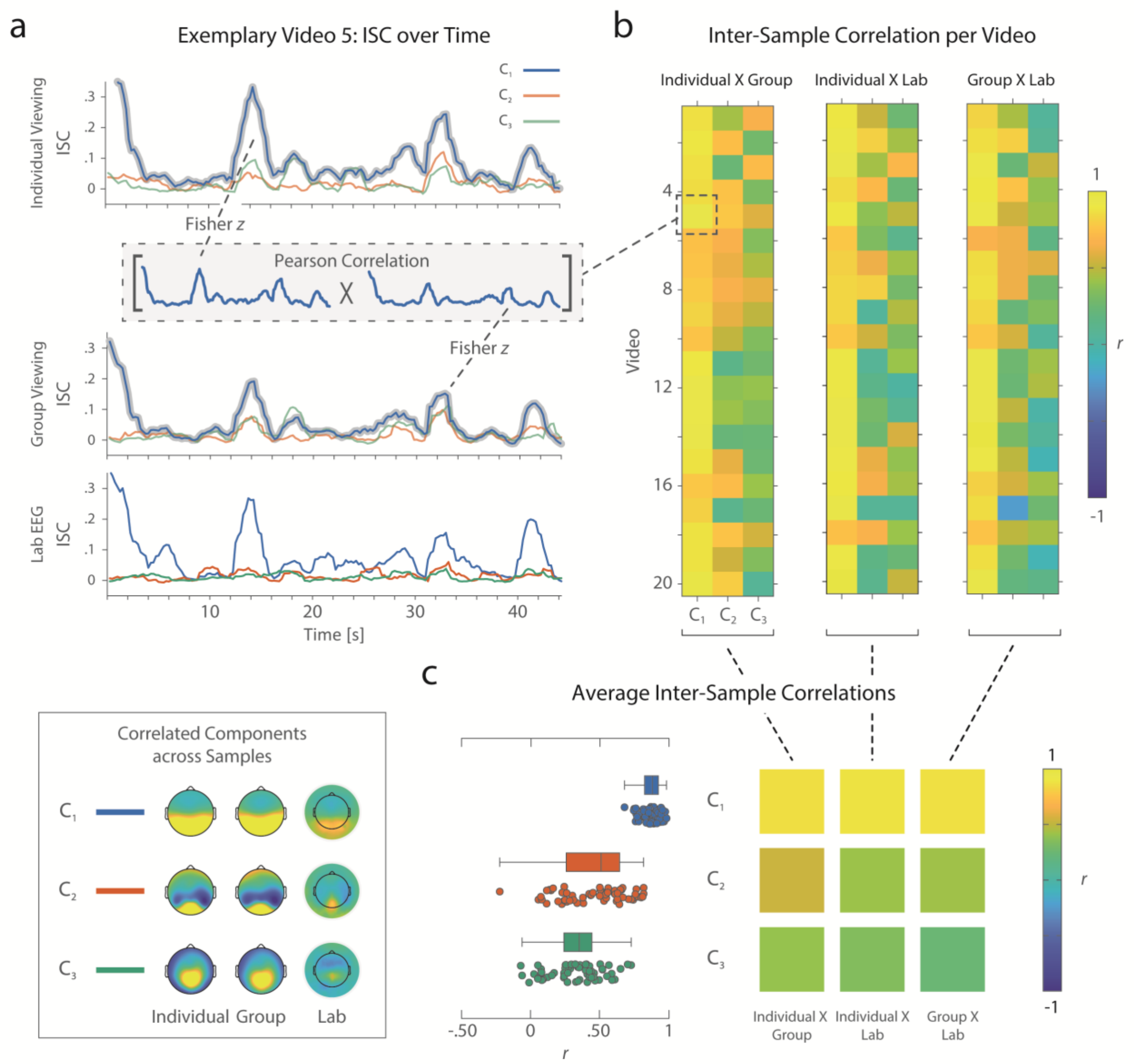

a
Exemplary Video 5: ISC over Time
Individual Viewing ISC
Fisher z
Pearson Correlation
X
Group Viewing ISC
Fisher z
Lab EEG ISC
Time [s]
b
Inter-Sample Correlation per Video
Individual X Group
Individual X Lab
Group X Lab
Video
r
c
Average Inter-Sample Correlations
Correlated Components across Samples
Individual
Group
Lab
Individual X Group
Individual X Lab
Group X Lab

Figure 4

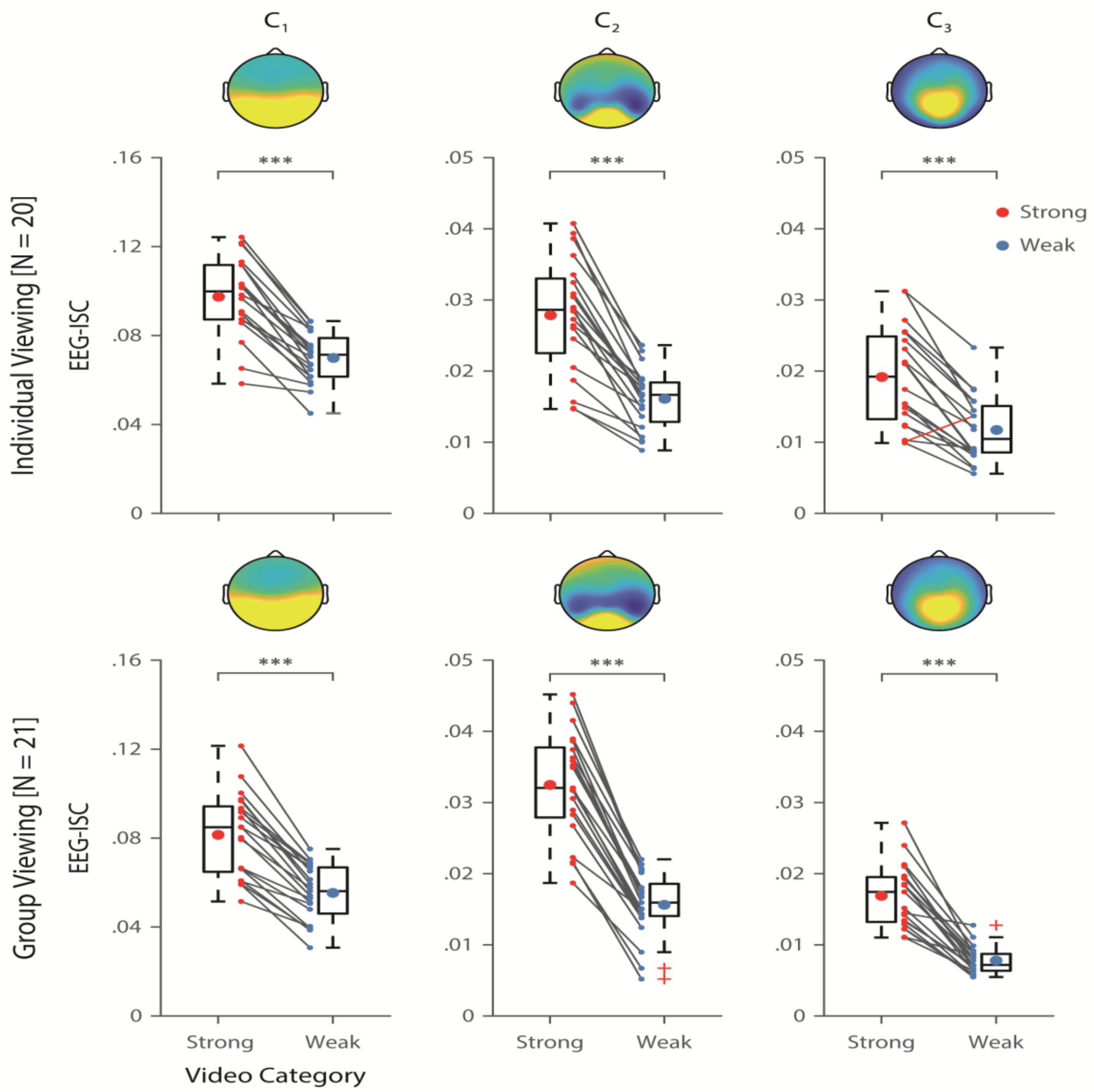

C1
C2
C3
Individual Viewing [N = 20]
Group Viewing [N = 21]
EEG-ISC
Strong
Weak
***
Video Category

Table 1 | *F*-statistics for Within and Between Subjects effects from mixed repeated measures ANOVA assessing differences across video categories and experimental tasks.

	Effect	F	p-value	Sum of Squares	η^2_G	η^2_p
C_1 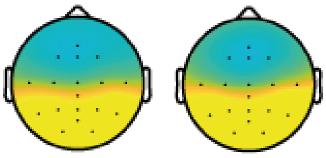	Video Category	278.36	<.0001	.0147	.44	.88
	Viewing Condition	11.23	.0018	.0048	.20	.22
	Video Category ✻ Viewing Condition	.19	.6657	< .0001	.	.
C_2 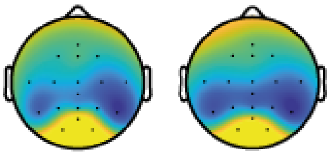	Video Category	381.58	<.0001	.0042	.58	.91
	Viewing Condition	1.30	.2616	< .0001	.	.
	Video Category ✻ Viewing Condition	12.11	.0012	.0001	.04	.24
C_3 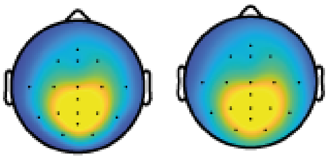	Video Category	162.18	<.0001	.0014	.44	.81
	Viewing Condition	5.39	.0256	.0002	.10	.12
	Video Category ✻ Viewing Condition	1.60	.2140	< .0001	.	.

Notes. *N* = 41. Within factor: "Video Category" (strong/weak). Between factor: "Viewing Condition" (Individual Viewing/Group Viewing). Type 3 Sums of Squares. η^2_G = generalized η^2; η^2_p = partial η^2. For ease of overview, effect sizes for effects with $p > .10$ are excluded.

Image Preview:

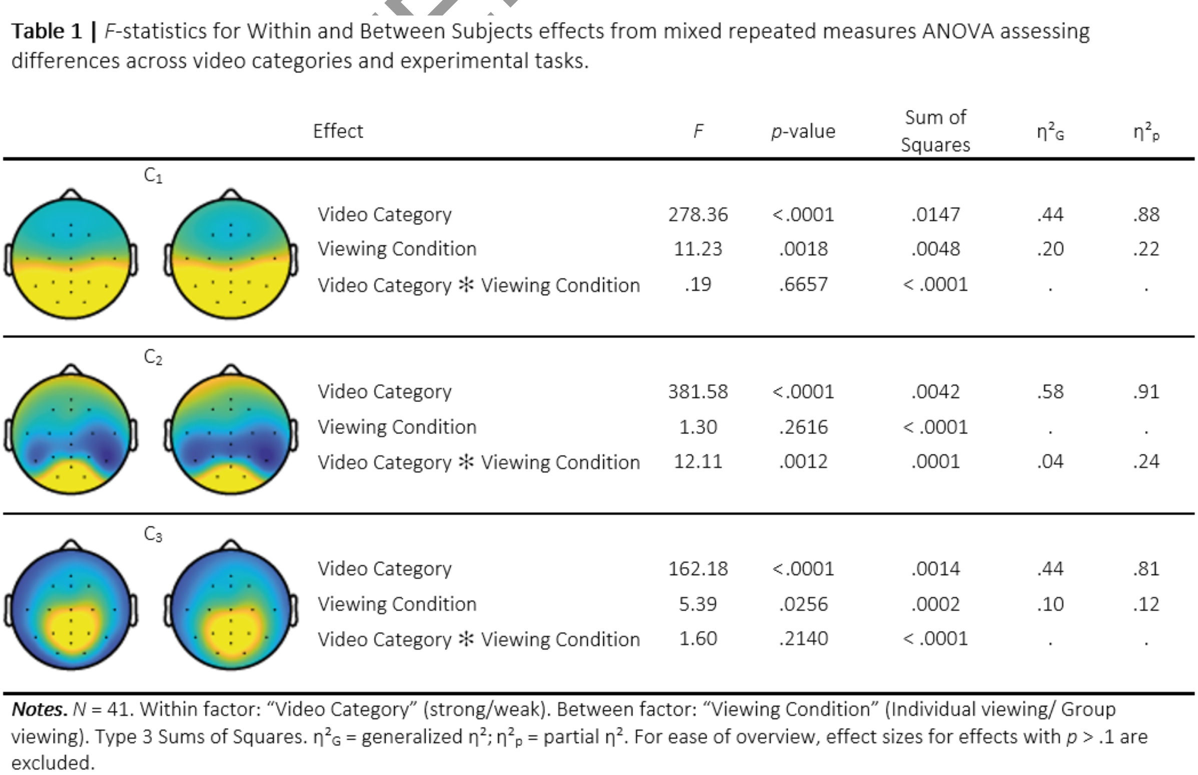
Table 1 | *F*-statistics for Within and Between Subjects effects from mixed repeated measures ANOVA assessing differences across video categories and experimental tasks.

	Effect	F	p-value	Sum of Squares	η^2_G	η^2_p
C_1	Video Category	278.36	<.0001	.0147	.44	.88
	Viewing Condition	11.23	.0018	.0048	.20	.22
	Video Category ✻ Viewing Condition	.19	.6657	< .0001	.	.
C_2	Video Category	381.58	<.0001	.0042	.58	.91
	Viewing Condition	1.30	.2616	< .0001	.	.
	Video Category ✻ Viewing Condition	12.11	.0012	.0001	.04	.24
C_3	Video Category	162.18	<.0001	.0014	.44	.81
	Viewing Condition	5.39	.0256	.0002	.10	.12
	Video Category ✻ Viewing Condition	1.60	.2140	< .0001	.	.

Notes. *N* = 41. Within factor: "Video Category" (strong/weak). Between factor: "Viewing Condition" (Individual viewing/ Group viewing). Type 3 Sums of Squares. η^2_G = generalized η^2; η^2_p = partial η^2. For ease of overview, effect sizes for effects with $p > .1$ are excluded.